Circuit-QED-based measurement of vortex lattice order in a Josephson junction array

R. Cosmic, Hiroki Ikegami, Zhirong Lin, Kunihiro Inomata, Jacob M. Taylor, and Yasunobu Nakamura

Phys. Rev. B **98**, 060501 — Published 21 August 2018

DOI: 10.1103/PhysRevB.98.060501

Circuit QED-based measurement of vortex lattice order in a Josephson junction array

R. Cosmic,[1,2,*] Hiroki Ikegami,[1,†] Zhirong Lin,[1] Kunihiro Inomata,[1,3]
Jacob M. Taylor,[4,5,2] and Yasunobu Nakamura[1,2,‡]

[1] *Center for Emergent Matter Science (CEMS), RIKEN, Wako, Saitama 351-0198, Japan*
[2] *Research Center for Advanced Science and Technology (RCAST), The University of Tokyo, Meguro-ku, Tokyo 153-8904, Japan*
[3] *National Institute of Advanced Industrial Science and Technology (AIST), Tsukuba, Ibaraki 305-8563, Japan*
[4] *Joint Center for Quantum Information and Computer Science (QuICS), University of Maryland, College Park, Maryland 20742, USA*
[5] *Joint Quantum Institute (JQI), National Institute of Standards and Technology, Gaithersburg, Maryland 20899, USA*

(Dated: August 1, 2018)

Superconductivity provides a canonical example of a quantum phase of matter. When superconducting islands are connected by Josephson junctions in a lattice, the low temperature state of the system can map to the celebrated XY model and its associated universality classes. This has been used to experimentally implement realizations of Mott insulator and Berezinskii–Kosterlitz–Thouless (BKT) transitions to vortex dynamics analogous to those in type-II superconductors. When an external magnetic field is added, the effective spins of the XY model become frustrated, leading to the formation of topological defects (vortices). Here we observe the many-body dynamics of such an array, including frustration, via its coupling to a superconducting microwave cavity. We take the design of the transmon qubit, but replace the single junction between two antenna pads with the complete array. This allows us to probe the system at 10 mK with minimal self-heating by using weak coherent states at the single (microwave) photon level to probe the resonance frequency of the cavity. We observe signatures of ordered vortex lattice at rational flux fillings of the array.

One of the central issues in modern physics is to elucidate the behavior of many-body systems. They are ubiquitous in nature, but our understanding is far from comprehensive because of difficulties in analytical and numerical calculations, especially for systems with frustration or those that exhibit the sign problem. Soon after the concept of building a controlled quantum system to emulate a less-understood system was suggested[1], several groups around the world began investigation of Josephson junction arrays (JJAs) formed in fabricated superconducting lattice structures as a way to explore ordered quantum matter[2–15]. More recently, the ability to control individual elements has enabled a proliferation of quantum simulation approaches[16–18] as demonstrated with ultracold neutral atoms[19,20], arrays of atomic ions[21], electrons in semiconductors[22], and superconducting circuits[23].

Here we show how the architecture of circuit quantum electrodynamics (cQED), so successful for qubit experiments, enables new observations of JJA-based many-body physics. Our system consists of a regular network of small superconducting islands coupled to each other via Josephson junctions [see Fig. 1(a)][2,3]. Interesting quantum many-body phenomena are expected as a result of competition between the Josephson energy E_J associated with the tunneling of Cooper pairs and the charging energy $E_C = e^2/(2C_J)$ describing the Coulomb blockade. (C_J is the capacitance between neighboring islands and e is elementary charge.) Indeed, low-frequency (DC) transport measurements have revealed that JJAs show a quantum phase transition between a superconducting and an insulating phases[6–8,10,12,13] and a commensurate-incommensurate transition of vortices in response to frustration induced by uniform external magnetic fields[9,11,24].

Circuit QED (cQED), a circuit implementation of a cavity QED, offers a novel approach to address such problems. It is a technique that has developed in the field of quantum information processing with superconducting qubits [25–27], where the strong coupling between an isolated dipole—typically a qubit—and cavity microwave photons allows for direct investigations of the dynamics of a qubit at the single-photon level. Applying this technique to the dynamics of many-body systems built from JJAs, we can investigate the ground states of JJAs with a weak perturbation of a single-photon level and directly detect dynamics of individual excitations. At the same time, we can avoid the self-heating from vortex induced phase slips. In this Letter, we report a cQED investigation of a JJA. Specifically, we observe the formation of lattice orderings of vortices via the response of the cavity. We find that the dynamics of the linearized response of the JJA—the plasma modes—leads to a strong shift of the cavity frequency in a manner that enables identification of ordered phases even with moderate disorder. These experiments represent a first step towards quantum many-body investigations, as we focus on the 'classical' regime where the Josephson energy is larger than the charging energy of individual islands, i.e., $E_J/E_C \approx 2$.

We use a JJA with a square network of superconducting islands arranged in a quasi-1D geometry of the length L of 30 plaquettes and the width W of 3 plaquettes (the area enclosed by one plaquette, S, is 6×6 μm^2), made of Al films evaporated on a silicon substrate. The JJA has $E_J/h = 25.8 \pm 0.2$ GHz estimated from the re-

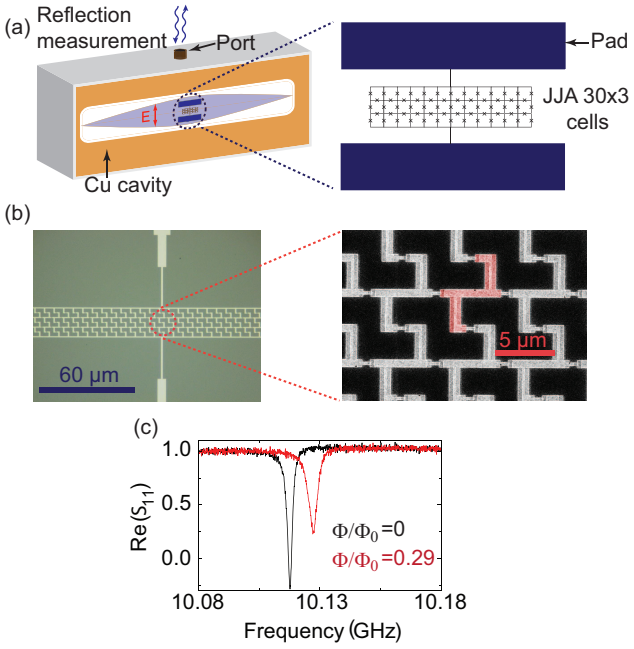

FIG. 1. (a) Schematic illustration of investigation of a JJA using the circuit QED architecture. The JJA consisting of 30×3 plaquettes connected to the two pads is mounted in a 3D microwave cavity. Response of the cavity is investigated by microwave reflection through the port. (b) Left: optical image of a JJA connected to the pads. Right: scanning electron microscope (SEM) image showing individual islands (false colored). Note the proximity along the lower left to upper right diagonal leads to additional capacitance, as discussed in the text. (c) Typical resonance spectra of the TE_{101} cavity mode for two different flux values. Φ/Φ_0 is the normalized flux threading each plaquette.

sistance of the junction using the Ambegaokar-Baratoff relation[28] and $E_C/h = 13$ GHz, corresponding to the nearest-neighbor capacitance C_J of 1.5 fF. We note that variations of E_J in individual junctions are estimated to be 5%, the impact of which is considered in the Supplemental Material[29]. In addition to the nearest neighbor capacitance, there is also a diagonal (next-nearest) capacitance along the upper-right axis of 120 aF [See right figure of Fig. 1(b)] and a capacitance between each island and ground of $C_g = 8$ aF. All capacitance parameters are estimated by the finite element calculations[29]. The JJA is connected to two large antenna pads [Fig. 1(b)] to allow for strong coupling to the modes of a 3D microwave cavity. The two pads in the cavity also form a capacitance of $C_S = 68.5$ fF ($E_{C_S}/2\pi \approx 250$ MHz). Note that, in our design, there is no Josephson junction on the top and bottom edges of the JJA shown in Fig. 1(a).

The JJA is placed in the center of a 3D cavity made of oxygen-free copper[30], where the strength of the electric field of the fundamental transverse electric (TE_{101}) mode with a bare frequency 10.127 GHz is strongest [Fig. 1(a)]. The coupling to the cavity is made by the two antenna pads connected to the JJA extending in the direction of the electric field of the TE_{101} mode. The pads provide a large electric dipole moment, allowing for a coupling strength of $g/2\pi \approx 100$ MHz. We measure the cavity's complex reflection coefficient S_{11}, see [Fig. 1(c)]. Photons enter and exit the cavity through the input port at a rate $\kappa_{\rm ext}/2\pi \approx 1.5$ MHz. The cavity containing the JJA is cooled down to ≈ 10 mK with a dilution refrigerator.

In order to study the frustration-induced properties of the JJA, we apply a magnetic field B normal to the JJA plane using a coil. Figure 2(a) shows $|S_{11}|$ for the JJA as a function of magnetic field and probe frequency. Here the magnetic field is expressed by the frustration parameter: a normalized flux per plaquette Φ/Φ_0, where $\Phi = SB$ is a flux threading in a plaquette and $\Phi_0 = h/2e$ is flux quantum (h is Plank's constant). The spectrum shown in the figure is symmetric around $\Phi/\Phi_0 = 1/2$ as expected, and exhibits structure near the fractional values of Φ/Φ_0 of 0, 1/9, 1/6, 1/3, 1/2, $\cdots$, as well as additional fine structure at non-fractional values of Φ/Φ_0. We note those structures corresponds to individual flux insertions. We also remark that the commensurate values listed above provide features also at 100 mK.

To understand the features observed, we consider the dual theory of the array, where we use vortices as our 'particle' rather than Cooper pairs. Specifically, in a uniform magnetic field, vortices have a chemical potential and are induced with a density of Φ/Φ_0. These vortices behave as particles with long-range interactions in a periodic potential made by the JJA pattern[31,32]. The vortices tunnel from site to site with a rate that scales with E_C and they interact strongly with a repulsive potential characterized by E_J. Our JJA with $E_J/E_C \approx 2 \gg 2/\pi$[233] suggests the predominance of the repulsive interaction, which allows for formation of vortex lattices commensurate with the underlying pattern of the JJA at the fractional Φ/Φ_0 as a result of the repulsion between vortices and the commensurability effect by the JJA pattern. The large shifts in the dip in reflection observed at around the fractional values of Φ/Φ_0 in Fig. 2(a) is one piece of evidence for such vortex-lattice formations.

To confirm the formation of vortex lattices, we numerically calculate the classical ground state of our problem, and capacitive terms are treated perturbatively in order to find the semi-classical response of the system. The Hamiltonian of the JJA is given by[3]

$$H_{\rm JJA} = \frac{(2e)^2}{2}\sum_{\langle i,j\rangle} n_i C_{ij}^{-1} n_j - E_J \sum_{\langle i,j\rangle} \cos(\phi_i - \phi_j - A_{ij}), \tag{1}$$

where n_i is the number of Cooper pairs and ϕ_i is a phase of the order parameter of the i-th island, satisfying the commutation relation $[\phi_j, n_k] = i\delta_{j,k}$. The first term in Eq.(1) represents the charging energy and the second term describes the Josephson effect, where C_{ij} is an element of a capacitance matrix $\mathbf{C}$ composed of C_J, C_S, and C_g[29] and $A_{ij} = (2\pi/\Phi_0)\int_i^j \mathbf{A}\cdot d\mathbf{l}$ is the line integral of

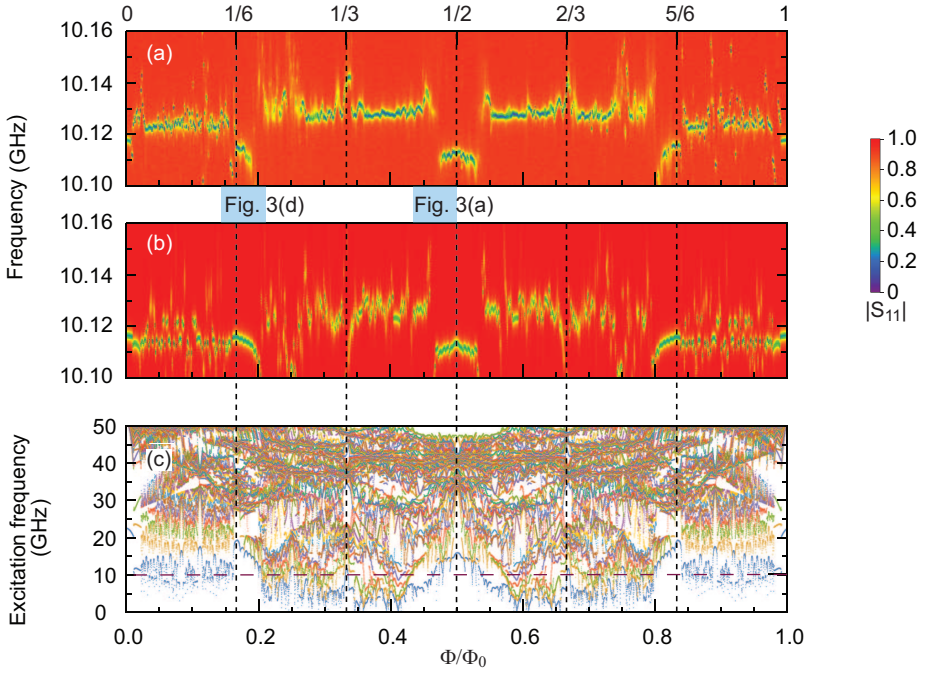

FIG. 2. (a) Experimental measurement of $|S_{11}|$ as a function of Φ/Φ_0 and probe frequency for the JJA of $E_J/E_C \approx 2.0$. The spectra are taken at 10 mK and at a power of $P_{\rm MW} = -132$ dBm (6.3×10^{-17} W) at the input port of the cavity, which corresponds to the average number of intracavity photons of 2.4. The cyan zones of the flux bias are magnified in Figs. 3(a) and (d). (b) Theoretical calculation of $|S_{11}|$ based upon the linear response theory of assuming fixed vortex configurations and no fitting parameters. (c) Plasma modes of the JJA as a function of Φ/Φ_0. Proximity of a plasma mode to the cavity frequency leads to the strong dispersive shift seen in (a). The horizontal dashed line indicates the bare cavity frequency.

the vector potential $\mathbf{A}$ from an island i to an island j. To find the ground state vortex configuration, i.e., the lowest classical-energy stable configuration of phases $\vec{\phi}^{(0)}$, we neglect any charging effect and numerically minimize the Josephson term $V_J(\vec{\phi}) = -E_J \sum_{\langle i,j \rangle} \cos(\phi_i - \phi_j - A_{ij})$ at a given Φ/Φ_0. [Here $\vec{\phi} = (\phi_1, \cdots, \phi_n)^{\rm T}$.] Note that, in this approximation, Eq.(1) reduces to the classical XY-spin model with a tunable frustration by A_{ij} and vortices correspond to classical ones. The obtained vortex configurations are identified by calculating the circulating current around each plaquette [cf. Figs. 3(a)(iv) and (b)(ii)] and show a periodic arrangement at fractional values of Φ/Φ_0. These periodic structures are stabilized to avoid the energy cost due to the vortex-vortex repulsion and the vortex-edge repulsion[9,11].

Once the vortex configurations of the ground states are known, the frequency of non-topological excitations ω_i can be evaluated in the presence of small E_C ($\ll E_J$). These excitations are plasma modes in the JJA or spin-wave modes in the language of the XY model. They are collective oscillations of $\vec{\phi}$ around $\vec{\phi}^{(0)}$ due to kinetic fluctuations in $\vec{\phi}$ associated with the charging energy. The mode frequencies are calculated by expanding $V_J(\vec{\phi})$ to second order

$$V_J(\vec{\phi}) = V_J(\vec{\phi}^{(0)}) + \frac{h_{ij}}{2}(\phi_i - \phi_i^{(0)})(\phi_j - \phi_j^{(0)}) \quad (2)$$

with $h_{ij} = \partial_{\phi_i}\partial_{\phi_j} V_J(\vec{\phi})\big|_{\vec{\phi}^{(0)}}$ and combining with the charging energy described in terms of $\mathbf{C}$. Then, a set of ω_i^2 are given as eigenvalues of $\left(\frac{2\pi}{\Phi_0}\right)^2 \mathbf{h}\mathbf{C}^{-1}$, where $\mathbf{h}$ is a matrix having elements h_{ij}. Note that $[\left(\frac{2\pi}{\Phi_0}\right)^2 \mathbf{h}]^{-1}$ can be regarded as an effective inductance matrix $\mathbf{L}$ of the JJA (see Supplemental Materials[29] for details).

For our regime of large E_J/E_C — the classical regime, the spin waves correspond entirely to the response of a network of inductors and capacitors, and thus are not chiral. The corrections to this behavior arise from voltage-induced twisted boundary conditions for the flux variables, exactly the effects that are exponentially suppressed in our transmon-like design. We anticipate that reducing E_J/E_C will lead to chiral effects in systems like ours.

The calculated spectra of the plasma modes are shown in Fig. 2(c). There are 63 modes in our JJA with 30×3 plaquettes for a given vortex configuration. The spectra steeply move and exhibit many discontinuous jumps with increasing Φ/Φ_0. The jumps are due to changes in the configuration of vortices induced by injections of

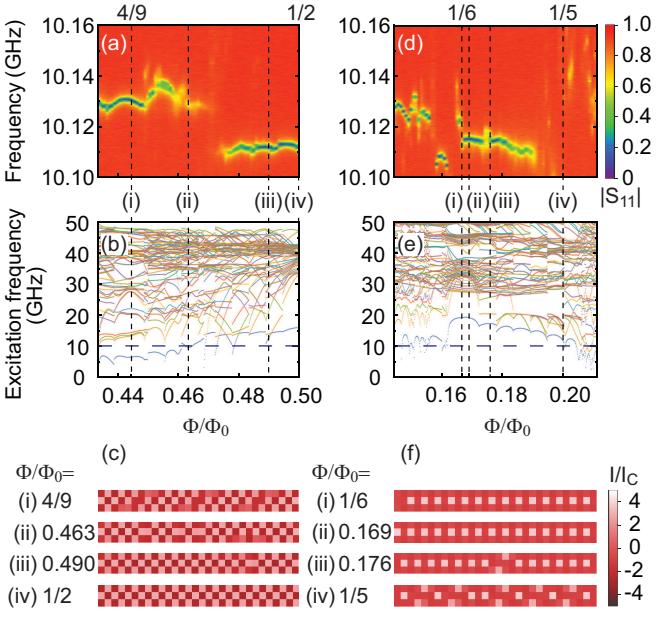

FIG. 3. Enlarged figures of the experimentally obtained $|S_{11}|$ and the calculated plasma modes shown in Fig. 2 around (a,b) $\Phi/\Phi_0 = 4/9$ through 1/2 and (d,e) 1/6 through 1/5. Calculated current circulation around each plaquette are shown in (c,f); Circulation near the maximum $I/I_C = 4$ is indicative of vortex locations, where I_C is the single junction critical current. Dashed lines in (a,b,d,e) correspond to the specific Φ/Φ_0 used in (c,f). We see individual vortex insertions from the theory are consistent with (a,d).

individual vortices. Remarkably, we see band structure with gaps at around $\Phi/\Phi_0 = 0$, 1/9, 1/6, 1/3, and 1/2 as a result of a repeated arrangement of vortices along the quasi-1D direction [see Fig. 2(c)], leading to an emergent super-cell and band-gap formation due to the associated Bloch theorem.

At the fractional values of Φ/Φ_0, the spectra occupy a wider range of Φ/Φ_0 without exhibiting a jump than the case of non-fractional values of Φ/Φ_0. This fact indicates the stability and the incompressibility of the commensurate vortex lattice. On the other hand, at non-fractional Φ/Φ_0, where vortices do not show a periodic arrangement, a vortex configuration can be easily changed when Φ/Φ_0 is varied because there are a number of similar configurations with an energy close to that of the ground state.

To understand the cavity response displayed in Fig. 2(a), we theoretically analyze it by considering the coupling to the plasma modes. The analysis is based on the following assumptions: (i) The plasma modes couple to cavity photons via a dipole charge induced on the pads. (ii) The coupling of the cavity photons to the input port is formulated by the input-output relation[34]. (iii) A small amount of ohmic loss in the Josephson junctions associated with the tunneling of quasiparticles is included. (See Supplemental Material for details of the theoretical analysis[29].) The calculated cavity response is compared with the experimental data in Fig. 2. We show there is a reasonable correspondence between them, especially a large frequency shift over a finite range of Φ/Φ_0 at around the fractional values of Φ/Φ_0.

We note that for regions where the lowest frequency spin-wave modes are dense and rapidly moving with flux, i.e., the incommensurate regions, we see poor qualitative agreement between the input-output theory and the experiment. We interpret this as due to a natural consequence of the 5% disorder in the array (see the Supplemental Material[29] for realizations of the theoretical spectra with different disorder); the need to include the quantum dynamics of the vortices, which are here entirely neglected; and the lack of inclusion of finite temperature corrections, where the system may be in a different, metastable vortex configuration some or all of the time. On the other hand, the ordered phases at the commensurate flux bias points are not affected even in the presence of the 5% disorder since these configurations are energetically stable (see the Supplemental Material[29].

At half vortex filling ($\Phi/\Phi_0 = 1/2$), we can plot the current around each plaquette from the theoretical calculation as shown in Fig. 3(c). Vortices are seen as peaks in circulation around individual plaquettes, and form a checkerboard. If we introduce one defect (by raising or lowering the magnetic field to create a vortex or anti-vortex, respectively), we see in the spin-wave response and in the reflection of the experiment a cusp at the insertion point of either a vortex or anti-vortex [see Figs. 3(a) and (b)]. However, one defect does not destroy the band gap observed in the spin-wave spectrum, which can be understood as a finite-size effect in the induced robustness of the checkerboard phase. Eventually, here around three anti-vortices, the spin wave spectrum begins to collapse and we observe a dramatic change in the cavity response, consistent with our qualitative interpretation of the destruction of rigidity in the vortex crystal. In principle, this rigidity is briefly recovered as we approach 4/9, which is again ordered, but has much lower fundamental frequency and is not as robust to single vortex subtraction.

Another key ordering occurs at 1/6 shown in Fig. 3(f), where we have alternating columns of empty columns and columns with one vortex in the middle. This is a quasi-1D phase, which with one anti-vortex added has appreciable compressibility[24]. However, with one vortex added, we see the onset of zig-zag ordering and expect these zig-zag excitations of a pair of vortices pushed towards the pads to have much smaller kinetic fluctuations than individual vortices. This persists down to 1/5 filling, where the addition of one more vortex leads to a compressible regime again [see Figs. 3(d) and (e)].

In conclusion, we have shown that cQED-based probing allows for the observation of low temperature phases of an engineered many-body superconducting system. While the present work has operated in the large capacitance regime, which suppresses the quantum dynamics

of the vortices, future work should be able to investigate a wider range of parameters and address key questions about the transition from vortex ordering to Cooper-pair hopping in a magnetic field[3]. This is particularly intriguing as, at low offset-charge disorder, the case of charged bosons with long-range interactions in a magnetic field naturally leads to fractional quantum Hall states[35]. Our approach may provide a framework for enabling such experiments.

We acknowledge M. Marthaler, J. Cole, N. T. Phuc, V. Sudhir, S. Furukawa , C. Lobb, and H. Mooij for fruitful discussions. JMT thanks the RIKEN team for their kind hospitality during his stays. This work was partly supported by ImPACT Program of Council for Science, Technology and Innovation and the NSF-funded Physics Frontier Center at the Joint Quantum Institute.

* cosmic@qc.rcast.u-tokyo.ac.jp
† hikegami@riken.jp
‡ yasunobu@ap.t.u-tokyo.ac.jp

[1] R. P. Feynman, Int. J. Theor. Phys. **21**, 467 (1982).
[2] R. Newrock, C. Lobb, U. Geigenmuller, and M. Octavio, in *Solid State Physics*, Vol. 54, edited by H. Ehrenreich and F. Spaepen (Elviser, 2000) pp. 263–512.
[3] R. Fazio and H. van der Zant, Phys. Rep. **355**, 235 (2001).
[4] E. Chow, P. Delsing, and D. B. Haviland, Phys. Rev. Lett. **81**, 204 (1998).
[5] D. Haviland, K. Andersson, P. Agren, J. Johansson, V. Schollmann, and M. Watanabe, Physica C **352**, 55 (2001).
[6] L. J. Geerligs, M. Peters, L. E. M. de Groot, A. Verbruggen, and J. E. Mooij, Phys. Rev. Lett. **63**, 326 (1989).
[7] H. S. J. van der Zant, F. C. Fritschy, W. J. Elion, L. J. Geerligs, and J. E. Mooij, Phys. Rev. Lett. **69**, 2971 (1992).
[8] H. S. J. van der Zant, W. J. Elion, L. J. Geerligs, and J. E. Mooij, Phys. Rev. B **54**, 10081 (1996).
[9] A. van Oudenaarden and J. E. Mooij, Phys. Rev. Lett. **76**, 4947 (1996).
[10] A. Rimberg, T. Ho, C. Kurdak, J. Clarke, K. Campman, and A. Gossard, Phys. Rev. Lett. **78**, 2632 (1997).
[11] A. van Oudenaarden, B. van Leeuwen, M. P. M. Robbens, and J. E. Mooij, Phys. Rev. B **57**, 11684 (1998).
[12] Y. Takahide, R. Yagi, A. Kanda, Y. Ootuka, and S.-i. Kobayashi, Phys. Rev. Lett. **85**, 1974 (2000).
[13] H. Miyazaki, Y. Takahide, A. Kanda, and Y. Ootuka, Phys. Rev. Lett. **89**, 197001 (2002).
[14] P. Delsing, C. Chen, D. Haviland, Y. Harada, and T. Claeson, Phys. Rev. B **50**, 3959 (1994).
[15] C. Chen, P. Delsing, D. Haviland, Y. Harada, and T. Claeson, Phys. Rev. B **54**, 9449 (1996).
[16] I. M. Georgescu, S. Ashhab, and F. Nori, Rev. Mod. Phys. **86**, 153 (2014).
[17] R. Blatt and C. F. Roos, Nat. Phys. **8**, 277 (2012).
[18] J. I. Cirac and P. Zoller, Nat. Phys. **8**, 264 (2012).
[19] I. Bloch, J. Dalibard, and S. Nascimbene, Nat. Phys. **8**, 267 (2012).
[20] H. Bernien, S. Schwartz, A. Keesling, H. Levine, A. Omran, H. Pichler, S. Choi, A. S. Zibrov, M. Endres, M. Greiner, V. Vuletić, and M. D. Lukin, Nature **551**, 579 (2017).
[21] J. Zhang, G. Pagano, P. W. Hess, A. Kyprianidis, P. Becker, H. Kaplan, A. V. Gorshkov, Z.-X. Gong, and C. Monroe, Nature **551**, 601 (2017).
[22] T. Hensgens, T. Fujita, L. Janssen, X. Li, C. Van Diepen, C. Reichl, W. Wegscheider, S. D. Sarma, and L. Vandersypen, Nature **548**, 70 (2017).
[23] J. Raftery, D. Sadri, S. Schmidt, H. E. Türeci, and A. A. Houck, Phys. Rev. X. **4**, 031043 (2014).
[24] C. Bruder, L. I. Glazman, A. I. Larkin, J. E. Mooij, and A. van Oudenaarden, Phys. Rev. B **59**, 1383 (1999).
[25] A. Blais, R.-S. Huang, A. Wallraff, S. M. Girvin, and R. J. Schoelkopf, Phys. Rev. A **69**, 062320 (2004).
[26] A. Wallraff, D. I. Schuster, A. Blais, L. Frunzio, R.-S. Huang, J. Majer, S. Kumar, S. M. Girvin, and R. J. Schoelkopf, Nature **431**, 162 (2004).
[27] J. Koch, T. M. Yu, J. Gambetta, A. A. Houck, D. I. Schuster, J. Majer, A. Blais, M. H. Devoret, S. M. Girvin, and R. J. Schoelkopf, Phys. Rev. A **76**, 042319 (2007).
[28] V. Ambegaokar and A. Baratoff, Phys. Rev. Lett. **10**, 486 (1963).
[29] See Supplemental Material (including Refs. [36–41]) at http://xxx for detailed information.
[30] H. Paik, D. I. Schuster, L. S. Bishop, G. Kirchmair, G. Catelani, A. P. Sears, B. R. Johnson, M. J. Reagor, L. Frunzio, L. I. Glazman, S. M. Girvin, M. H. Devoret, and R. J. Schoelkopf, Phys. Rev. Lett. **107**, 240501 (2011).
[31] A. Larkin, Y. Ovchinnikov, and A. Schmid, Physica B: Cond. Matt. **152**, 266 (1988).
[32] U. Eckern and A. Schmid, Phys. Rev. B **39**, 6441 (1989).
[33] R. Fazio and G. Schön, Phys. Rev. B **43**, 5307 (1991).
[34] D. F. Walls and G. J. Milburn, *Quantum Optics* (Springer, Berlin, 1994).
[35] M. C. Diamantini, P. Sodano, and C. Trugenberger, Nucl. Phys. B **474**, 641 (1996).
[36] A. A. Clerk, M. H. Devoret, S. M. Girvin, F. Marquardt, and R. J. Schoelkopf, Rev. Mod. Phys. **82**, 1155 (2010).
[37] M. D. Reed, L. DiCarlo, B. R. Johnson, L. Sun, D. I. Schuster, L. Frunzio, and R. J. Schoelkopf, Phys. Rev. Lett. **105**, 173601 (2010).
[38] W. Elion, J. Wachters, L. Sohn, and J. Mooij, Phys. Rev. Lett. **71**, 2311 (1993).
[39] A. van Oudenaarden, S. Várdy, and J. Mooij, Phys. Rev. Lett. **77**, 4257 (1996).
[40] A. Larkin, Y. N. Ovchinnikov, and A. Schmid, Physica B: Condensed Matter **152**, 266 (1988).
[41] S. Korshunov, Physica B: Condensed Matter **152**, 261 (1988).